Astron. Astrophys. 331, 1119–1129 (1998)

ASTRONOMY AND ASTROPHYSICS

The Hipparcos proper motion link to the extragalactic reference system using NPM and SPM⋆

I. Platais[1], V. Kozhurina-Platais[1], T.M. Girard[1], W.F. van Altena[1], C.E. López[2], R.B. Hanson[3], A.R. Klemola[3], B.F. Jones[3], H.T. MacGillivray[4], D.J. Yentis[5], J. Kovalevsky[6], and L. Lindegren[7]

[1] Department of Astronomy, Yale University, P.O. Box 208101, New Haven, CT 06520-8101, USA
[2] Felix Aguilar Observatory and Yale Southern Observatory, San Juan, Argentina
[3] UCO/Lick Observatory, University of California, Santa Cruz, CA 95064, USA
[4] Royal Observatory, Blackford Hill, Edinburgh EH9 3HJ, UK
[5] Department of the Navy, Naval Research Laboratory, Washington, DC 20375, USA
[6] CERGA, Observatoire de la Côte d'Azur, Avenue Copernic, F-06130 Grasse, France
[7] Lund Observatory, Box 43, S-22100 Lund, Sweden

Received 13 August 1997 / Accepted 11 November 1997

Abstract. We describe the use of the Lick Northern Proper Motion (NPM) program and its southern-sky complement, the Yale/San Juan Southern Proper Motion (SPM) program, to determine the Hipparcos proper motion link to the extragalactic reference system defined by galaxies. In total ∼9,100 Hipparcos stars were chosen for the NPM link solution and ∼4,100 for the SPM solution. The typical accuracy of the NPM absolute proper motions is 5 mas yr^{-1}. For the SPM proper motions it varies from 2 to 4 mas yr^{-1}. The link solutions indicate a presence of magnitude equation in both the NPM and SPM. In the case of the NPM three different approaches (i.e., introducing a magnitude cutoff, additional linear magnitude terms, and including a fictitious zone of avoidance) were examined to alleviate the magnitude equation problem. The SPM proper motions show a notable correlation between the postfit residuals and the size of the magnitude equation correction applied. It is quite likely that galaxies have a magnitude equation different from that affecting the stellar images. We note an improvement in the spin solution with re-calibrated galaxy magnitudes and, subsequently, changed magnitude-equation corrections for the galaxies.

Key words: astrometry – catalogs – reference systems – methods: data analysis

1. Introduction

The ESA Hipparcos mission has provided high precision stellar positions, proper motions, parallaxes and magnitudes for 118,000 stars and a few other celestial objects. Due to the chosen scheme of measurements and the lack of appropriate reference objects, the provisional Hipparcos positions and proper motions (labeled as the H37C catalogue) were essentially in an arbitrarily chosen reference system. Thus, the preliminary Hipparcos proper motions contained a small net rotation about an arbitrary axis. One way of detecting this spin is to compare the absolute proper motions from a photographic survey, calibrated relative to distant galaxies, to the H37C proper motions (Lindegren & Kovalevsky 1995). The obvious advantage of such an approach is a large number of common stars which can be used.

The Lick Observatory NPM program and the Yale/San Juan SPM program, which together cover the whole sky, are well-suited for the purpose of determining the Hipparcos proper-motion link. The Lick NPM1 Catalog (Klemola et al. 1993) contains a relatively small fraction of the Hipparcos Input Catalogue (HIC) stars (Turon et al. 1992) or about 18% of the HIC stars at $\delta > -23°$. This incompleteness is compensated by an excellent sky coverage from the North celestial pole down to $\delta = -23°$, except for the galactic zone of avoidance. In contrast, the Yale/San Juan SPM fields measured thus far (as of February 1996) cover only about 2,000 square degrees on the sky but include virtually all HIC stars (over 4,000) in that area. The two programs have similar plate material, although differ, for example, in the grating image and the short & long exposure separation, and the data measurement and reduction procedure. The NPM proper motions are derived just from blue-plate pairs, whereas the SPM has also visual-plate pairs.

The purpose of this study is to provide a detailed analysis of the NPM and SPM contributions to the Hipparcos proper-motion link used by Kovalevsky et al. (1997) in the final proper-motion link synthesis. In particular, possible sources of systematic errors in the NPM and SPM were scrutinized and an attempt

Send offprint requests to: I. Platais

⋆ Based on observations made with the ESA Hipparcos satellite

was made to minimize the effect of systematics in the spin solution. Basic results of the NPM and SPM contributions were also reported at the Hipparcos Venice '97 symposium (Platais et al. 1997).

2. Lick NPM contribution

2.1. NPM scope and link solution

The Lick NPM1 Catalog (Klemola et al. 1993), contains 149,000 stars, with $8 \lesssim B \lesssim 18$, from 899 NPM fields north of $\delta = -23°$. The mean number of galaxies per field is 80. The rms precision of the NPM1 absolute proper motions is 5 mas yr^{-1} (Klemola et al. 1994). The NPM1 data have been extensively tested (Klemola et al. 1987, 1994; Hanson 1995, private communication) and found to be free of systematic errors for the faint stars ($B > 12$) on which the galactic structure and kinematic studies have been based.

The NPM1 Catalog contains over 13,400 Hipparcos stars, and is thus by far the largest source of data for the Hipparcos proper-motion link. However, 96% of the NPM1 Hipparcos stars have $B < 12$. Consequently, the Hipparcos link comparison represents the first systematic test of the NPM1 proper motions at such bright magnitudes. Any magnitude-dependent systematic errors in the NPM1 bright stars' data may limit the number of stars which can be used in the Hipparcos link, or even vitiate the link itself.

Preliminary comparisons of proper motions in H37C and the NPM1 indicated a linear magnitude equation of about 1 mas yr^{-1} mag^{-1} in the NPM1 data at least down to $B = 11$ (see Fig. 1). The magnitude equation appears to be coordinate-independent, although in declination it shows a different slope for stars located north or south of $\delta = -2\overset{\circ}{.}5$.

In principle the NPM1 magnitude equation could be eliminated *internally* using the grating-image offset modeling technique (Jefferys 1962). However, this cannot be accomplished with the existing NPM blue plate measurements. As Klemola et al. (1971, Fig. 2) illustrated, the Lick automatic measuring machine was restricted to a range of ∼4 mag about the optimum magnitude for each image system. The NPM plates were taken with a 4-mag objective grating. Consequently, it was not possible to measure *both* the zero-order and higher-order grating images on either (long or short) exposure. Moreover, as Klemola et al. (1987) described, the offset between the long and short exposures (∼1 mm) is so small that for $B \lesssim 9$ the greatly-overexposed long-exposure image encroaches onto the short exposure. Because of this problem, *no* short-exposure grating image measurements were used for NPM1. Thus, for $B \lesssim 10$, the NPM1 proper motions were measured using the short-exposure zero-order images only (see Klemola et al. 1971, Fig. 2). These images are progressively more overexposed for brighter magnitudes, which may well be the cause of the effects seen in Fig. 1.

The NPM1 bright stars' magnitude equation could be corrected *externally* by comparison with some other catalogues. However, there are no other absolute proper motions available which could be readily used to correct the magnitude equation for the bright stars to the accuracy required. Since the spin components are correlated with the magnitude equation, we did not attempt to correct the magnitude equation in the NPM1 Catalog using the H37C itself.

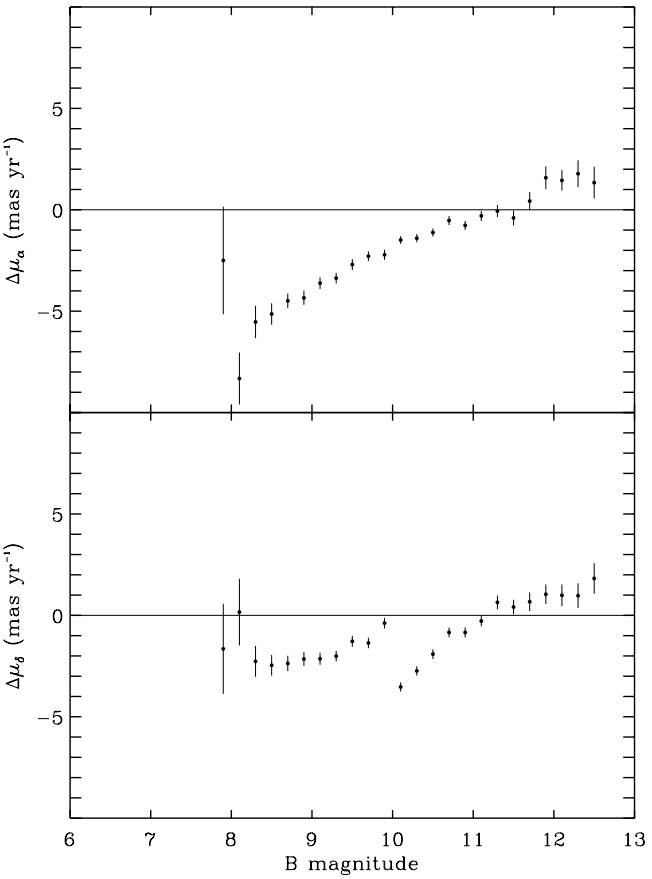

Fig. 1. Binned Hipparcos (H) *minus* NPM proper motions as a function of B magnitude. Error bars indicate the error of the mean in each magnitude bin. The NPM proper motions have a more pronounced magnitude equation in μ_δ for bright stars with $\delta < -2\overset{\circ}{.}5$ and, thus, these low declination stars have been excluded for $B < 10$. This explains the break in the $\Delta\mu_\delta$ plot at $B = 10$.

The definition of the proper-motion link equations, representing a small rigid-body rotation, is given for instance by Lindegren & Kovalevsky (1995). In accordance with this definition, an arbitrary spin can be split into three orthogonal rotations about the X,Y,Z axes: ω_x (X-axis towards $\alpha = 0^h$, $\delta = 0°$), ω_y (Y-axis towards $\alpha = 6^h$, $\delta = 0°$) and ω_z (Z-axis towards $\delta = 90°$)

$$\begin{aligned} \Delta\mu_\alpha \cos\delta &= -\omega_x \cos\alpha \sin\delta - \omega_y \sin\alpha \sin\delta + \omega_z \cos\delta \\ \Delta\mu_\delta &= +\omega_x \sin\alpha - \omega_y \cos\alpha \end{aligned} \quad (1)$$

where $\Delta\mu$ is in the sense 'Hipparcos − NPM'. Note that henceforth all calculations and numerical results are referenced to the final adopted system of the Hipparcos proper motions (Kovalevsky et al. 1997). For the sake of uniformity the Hipparcos proper motions were transformed from the J2000 equator to the B1950 equator relative to which the NPM proper motions

Table 1. Residual spin components from the solutions with NPM & SPM data

Data	$\Delta\mu$	$\omega_x \pm \epsilon_x$	$\omega_y \pm \epsilon_y$	$\omega_z \pm \epsilon_z$	$d_0 \pm \epsilon_0$	$d_1 \pm \epsilon_1$	N_H	σ
NPM	$\mu_\alpha \cos\delta$	+0.09±0.18	–0.20±0.18	+1.46±0.30	–5.11±0.28	+1.58±0.06	9161	6.1
NPM[a]	$\mu_\alpha \cos\delta$	+0.70 0.26	–0.03 0.31	–1.93 0.09	—	—	5748	6.2
NPM[b]	μ_δ	–0.32 0.11	–0.18 0.10	—	–2.06 0.11	+1.23 0.07	7660	6.0
NPM[a,b]	μ_δ	+0.16 0.18	+0.04 0.12	—	—	—	4409	6.3
SPM_B	$\mu_\alpha \cos\delta$	+0.23 0.13	+0.50 0.20	0.00 0.08	—	—	4042	3.8
SPM_V	$\mu_\alpha \cos\delta$	+0.44 0.12	+0.71 0.18	–0.30 0.07	—	—	4067	3.4
SPM_B	μ_δ	+0.07 0.15	+0.58 0.08	—	—	—	3751	4.0
SPM_V	μ_δ	+0.30 0.12	+0.76 0.06	—	—	—	4094	3.4

[a] Fictitious zone of avoidance added
[b] Only stars with $\delta > -2\overset{\circ}{.}5$ used

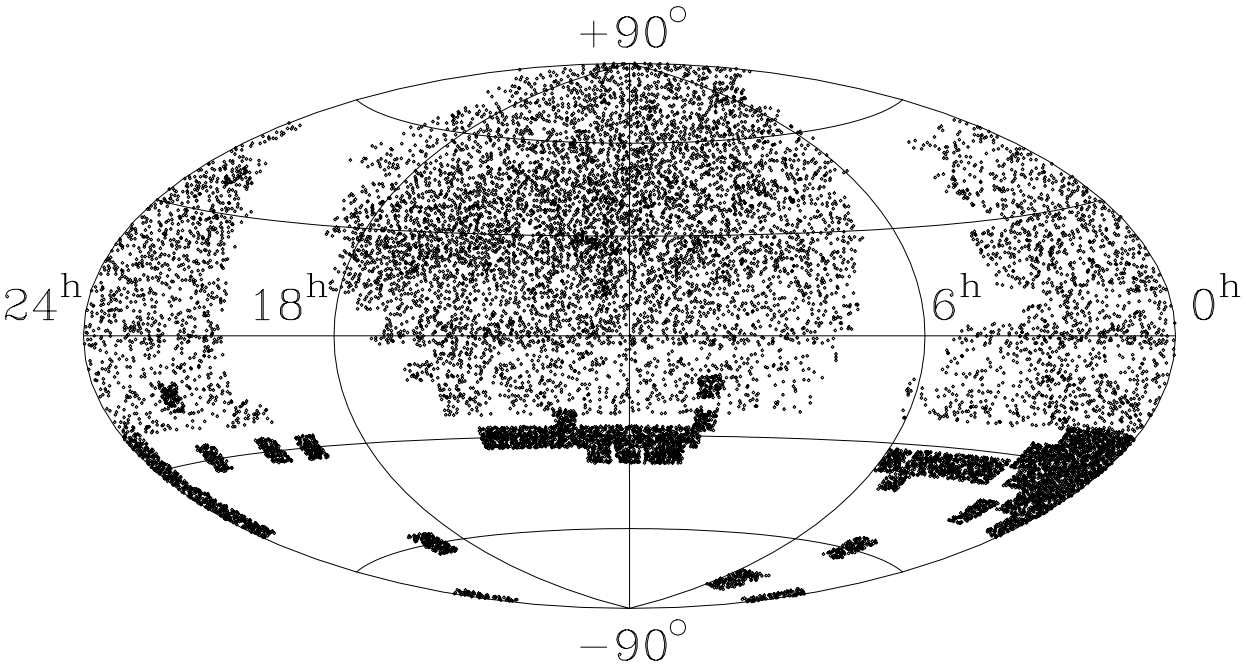

Fig. 2. Sky distribution of the selected Hipparcos stars in NPM1 Catalog (light gray) and the Yale/San Juan SPM Hipparcos stars (dark gray).

are given. Eqs. (1) can be solved together using least-squares adjustment, however, we separated them because the systematics have a different signature in right ascension as opposed to declination. The first trial solutions using the NPM data also indicated that the bright southern declination stars ($\delta < -2\overset{\circ}{.}5$) significantly distort the link solution. Therefore, it was decided to use these low declination stars only if they are fainter than B = 10. This resulted in ∼9,200 NPM stars for the spin solution shown in Fig. 2.

2.2. Magnitude-equation consequences on the link

Based upon awareness of the magnitude equation in the NPM proper motions we explored three possible ways to reduce the impact of magnitude equation on the link solution.

Firstly, in the solution one may use only relatively faint stars (e.g. $B > 10.5$), anticipating that the magnitude equation vanishes at some magnitude. A set of spin calculations at different magnitude cutoffs shows that the solution using fainter stars is improving, however, it cannot be said with confidence at what magnitude the Hipparcos stars in the NPM1 Catalog are indeed magnitude-equation free. The so-called Heidelberg solution (Kovalevsky et al. 1997) provides a number of solutions at different magnitude cutoffs. They indicate rather weak dependence on the chosen cutoff for ω_x and ω_y and, thus, suggest a judicious trimming will produce a reasonable solution. The third component, ω_z, cannot be reliably determined from the NPM data due to high sensitivity to the exact value of the cutoff. We conclude that this sample trimming approach is not

entirely useful, although it could be if more common stars were available. It is unfortunate that more of the fainter stars originally proposed to link with the NPM were not included in the Hipparcos Input Catalogue.

Secondly, despite the correlations it seems feasible to supplement the conventional rotation equations with a linear magnitude equation term, $d_0 + (m - 9)d_1$, where m is the star's magnitude. This term essentially allows us to find a magnitude equation in the NPM proper motions using directly the Hipparcos data. Indeed, we noticed a substantial improvement of the solution. This procedure would be ideal except for the fact that the correlations between the spin components and the magnitude equation cannot be disentangled unambiguously. For this reason a third way of handling the magnitude equation is proposed.

A careful inspection of how the magnitude equation effects the spin components implies the significance of the star distribution over the sky. The key factor to minimize the effect of a *coordinate-independent* magnitude equation on link solution is to seek a well-balanced distribution of the stars. In other words, for the spin components ω_x and ω_y the stars must be distributed such that the sums of the corresponding geometrical weighting factors in the link equation (see Eq. 27 in Lindegren & Kovalevsky 1995) are close to zero. This symmetry requirement is not necessary for the third component, ω_z, which is so strongly correlated with the magnitude equation in right ascension that it makes ω_z ill-determined.

To achieve the desired distribution of the NPM1 Catalog stars it was modified by introducing a 44°-wide fictitious zone of avoidance perpendicular to the galactic plane. In addition, the stars with both $\delta < -2.5$ and $B < 10$ were deleted from the sample in order to reduce further the effect of magnitude-equation slope change in the southern hemisphere.

The results of various NPM spin solutions are shown in Table 1, where $\Delta\mu$ indicates which proper-motion component differences were used in the solution; ω_x, ω_y and ω_z are the spin components with their formal error estimates from least-squares solution; d_0 and d_1 are the coefficients of the linear magnitude equation as defined above, with units of mas yr^{-1}; N_H is the number of Hipparcos stars used and σ is the standard deviation of the post-fit residuals. The NPM spin solution with a linear magnitude term included shows important corrobative evidence to the statement in Sect. 2.1, i.e., the NPM1 Catalog is systematic error free for $B > 12$. In this solution the magnitude term, $d_0 + (m - 9)d_1$, is equal to zero at $B = 12.2$, quite close to the predicted value.

The full correlation matrix C^N is given for the right ascension solution (first line in Table 1) – the only NPM solution used in the link synthesis (Kovalevsky et al. 1997). The order of the elements in matrix C^N follows the term sequence ω_x, ω_y, ω_z, d_0 and d_1.

$$C^N = \begin{pmatrix} 1.00 & -0.02 & +0.34 & -0.41 & +0.02 \\ & 1.00 & -0.02 & 0.00 & -0.01 \\ & & 1.00 & -0.93 & -0.01 \\ & & & 1.00 & -0.27 \\ & & & & 1.00 \end{pmatrix} \quad (2)$$

In general, the matrix C^N elements show small correlations due to an uneven distribution of the Hipparcos stars, except for C^N_{34} which numerically confirms the high degree of correlation between ω_z and d_0. On the other hand, C^N_{35} indicates essentially zero correlation between ω_z and d_1. It means that the slope, produced by magnitude equation, does not affect the link (although it contributes to the link formal error), whereas the offset part, d_0, is directly associated with the spin components.

3. Yale/San Juan SPM contribution

The Yale/San Juan SPM program is an extension of the Lick Observatory Northern Proper Motion program south of $\delta = -17°$. A brief description of the SPM goals, plate material, input catalogue preparation and measurements can be found in van Altena et al. (1990), Platais et al. (1992, 1993, 1995) and Girard et al. (1998). Here we give the SPM reduction overview which illuminates some critical aspects of the link.

3.1. SPM plate material & reduction procedure

The SPM plates, taken on ∼5° centers, cover $6\overset{\circ}{.}3 \times 6\overset{\circ}{.}3$ areas on the sky with the plate scale $55\overset{\prime\prime}{.}1$ mm^{-1}. Each field is taken with a 3.5-mag objective grating, two-hour exposure and an offset two-minute exposure on pairs of visual and blue plates at two different epochs about 20 years apart. The plates are scanned in the object-by-object mode with the Yale PDS 2020G microdensitometer equipped with laser-interferometer encoders which ensure submicron measuring precision. The grating images through second order are centered using a two-dimensional Gaussian fit. The stars and galaxies fainter than $V \approx 14$ have only a single image on the SPM plates.

The SPM reduction flow-chart is described by Girard et al. (1998) and will be discussed in detail elsewhere. Here we only mention the main steps of the reduction procedure.

- On each plate various grating images and both exposures are transformed into the long exposure zero-order image system. This involves a careful account for the magnitude-dependent effects (i.e. magnitude equation) in the coordinates. Also, BV magnitudes are derived in addition to the astrometric reductions. The Yale CCD BV calibrating sequences are centered on the faintest star in each sequence from the Guide Star Photometric Catalog (Lasker et al. 1988).
- The relative proper motions are derived from the plate-pair solution using faint anonymous reference stars and a polynomial plate model. Usually 1,000 to 1,500 such stars are available. The blue and visual plate pairs are reduced separately.

Table 2. Hipparcos-SPM spin post-fit residuals

SPM field	Field center α (1950)	δ	Blue-plate pair N_H	$\langle\Delta\mu_\alpha\rangle$	$\langle\Delta\mu_\delta\rangle$	σ_α	σ_δ	Visual-plate pair N_H	$\langle\Delta\mu_\alpha\rangle$	$\langle\Delta\mu_\delta\rangle$	σ_α	σ_δ
28	0^h00^m	$-75°$	97	-0.68	0.01	4.0	4.9	105	-0.08	-1.28	3.3	3.2
33	5 00	−75	70	-0.24	—	3.8	5.4	87	-2.22	—	3.4	3.4
124	3 36	−60	98	-0.25	0.01	4.1	5.6	101	0.56	-0.35	2.7	3.3
150	19 12	−60	110	0.28	-0.88	3.9	4.3	114	-0.84	0.68	3.1	2.7
263	0 00	−45	98	1.31	-2.17	4.4	5.4	110	-0.23	-1.81	3.6	3.5
264	0 24	−45	97	-1.19	-2.77	3.8	4.0	98	-1.18	-2.47	4.2	4.0
268	2 00	−45	103	-0.28	-1.19	3.9	3.6	107	-1.02	-0.04	3.0	3.1
322	23 36	−45	116	1.36	-2.08	3.3	4.3	118	3.24	-0.80	3.4	4.0
323	0 00	−40	107	0.00	0.07	3.9	3.8	107	-2.02	0.54	2.9	3.1
324	0 24	−40	93	-2.72	1.51	3.5	3.4	92	-1.70	0.67	3.2	3.6
325	0 48	−40	95	1.23	-2.34	5.0	4.9	94	2.29	-1.25	3.7	3.7
326	1 12	−40	103	-0.73	1.53	3.8	4.4	105	0.16	1.11	3.1	2.8
336	5 12	−40	78	1.82	0.02	3.4	4.2	79	1.37	1.73	2.7	2.3
382	23 36	−40	61	-2.48	3.16	5.3	5.8	93	-2.29	0.47	3.8	3.7
383	0 00	−35	92	—	-0.18	3.8	5.3	99	0.88	-0.08	3.6	3.4
384	0 20	−35	105	-0.69	-0.39	4.1	3.5	107	1.90	-1.30	3.7	3.4
385	0 40	−35	87	-0.01	0.04	3.7	4.1	93	1.23	-0.73	3.2	3.9
386	1 00	−35	85	0.02	-0.63	4.7	4.3	87	0.23	0.85	3.3	3.0
387	1 20	−35	81	-0.45	0.17	4.5	4.1	90	-1.56	-0.49	3.1	3.5
388	1 40	−35	92	1.88	-1.35	3.6	3.5	93	-0.24	-0.92	3.5	3.0
389	2 00	−35	95	1.47	-0.90	3.1	3.7	97	3.06	1.28	4.3	3.2
392	3 00	−35	84	-0.51	0.49	3.9	3.8	83	1.62	1.24	2.9	3.4
393	3 20	−35	87	0.12	—	3.8	3.7	89	-0.02	-0.68	3.7	4.3
394	3 40	−35	83	-1.30	1.77	3.3	4.2	89	0.76	1.18	3.0	3.1
395	4 00	−35	84	0.06	0.68	4.1	3.2	89	-1.50	1.31	3.7	2.8
396	4 20	−35	92	0.88	—	3.7	3.7	93	—	-0.10	2.8	2.7
397	4 40	−35	71	1.41	—	3.3	4.3	75	1.55	-0.27	2.4	3.5
398	5 00	−35	76	0.43	-1.09	4.7	4.5	84	-0.62	-1.44	2.9	3.0
416	11 00	−35	91	-0.24	-0.44	4.2	4.1	107	-1.93	-2.90	3.5	3.2
417	11 20	−35	106	-1.59	-2.69	3.6	3.8	106	-0.47	-1.17	3.9	3.3
419	12 00	−35	90	-2.25	0.90	4.3	3.9	89	2.56	-3.88	3.6	3.2
421	12 40	−35	82	0.82	-1.49	3.7	3.3	80	-0.98	-0.30	2.8	3.4
454	23 40	−35	93	-0.40	-0.07	3.5	2.6	93	0.80	-1.75	3.7	3.6
455	0 00	−30	96	0.41	-0.08	3.8	3.1	102	0.45	-1.23	3.8	3.1
456	0 20	−30	102	-0.05	0.08	4.2	5.0	99	1.14	0.74	3.9	3.1
457	0 40	−30	105	-2.69	-1.05	3.4	4.0	102	—	-2.27	3.0	3.2
458	1 00	−30	91	-0.49	-0.10	4.4	3.8	95	1.11	-0.17	3.4	3.1
459	1 20	−30	102	-0.60	-0.96	4.4	3.8	101	-1.76	-0.76	3.0	3.5
460	1 40	−30	88	0.82	—	3.9	4.1	93	0.11	-1.00	3.3	2.9
461	2 00	−30	88	-1.11	-0.99	4.7	6.1	102	0.67	-1.04	4.2	3.4
489	11 20	−30	90	0.83	0.01	3.8	3.5	94	1.51	-0.31	2.6	2.3
490	11 40	−30	82	-2.59	0.98	3.4	3.6	82	-0.79	0.30	3.3	2.6
491	12 00	−30	74	-0.13	-1.74	3.0	3.6	73	1.96	-0.71	3.3	2.9
492	12 20	−30	83	0.74	-3.15	3.3	3.9	85	—	-1.21	3.1	2.9
493	12 40	−30	77	1.16	1.03	3.7	4.5	81	-1.55	-2.28	3.2	3.7
494	13 00	−30	99	1.12	-1.86	3.4	3.7	96	0.29	-0.59	3.2	2.9
495	13 20	−30	53	-1.58	0.83	3.9	3.4	85	—	—	3.5	2.4
496	13 40	−30	92	-0.86	1.16	4.6	4.6	97	0.88	2.59	3.2	3.5
497	14 00	−30	101	2.13	-1.24	3.6	3.8	100	0.91	-0.90	4.0	4.4
513	19 20	−30	86	-0.70	—	4.2	3.9	90	—	—	4.0	3.9
516	20 20	−30	104	0.37	0.52	4.1	3.4	104	-0.04	-0.39	3.1	3.3
521	22 00	−30	90	0.92	-0.70	3.5	3.0	90	-1.22	-3.20	3.5	3.2

Table 2. (continued)

SPM field	Field center α (1950)	δ	Blue-plate pair N_H	$\langle\Delta\mu_\alpha\rangle$	$\langle\Delta\mu_\delta\rangle$	σ_α	σ_δ	Visual-plate pair N_H	$\langle\Delta\mu_\alpha\rangle$	$\langle\Delta\mu_\delta\rangle$	σ_α	σ_δ
526	23 40	−30	94	—	-1.52	4.6	4.0	99	-1.47	-2.49	3.6	3.5
527	0 00	−25	89	-1.85	1.74	4.2	4.4	92	-0.45	1.65	4.0	3.3
528	0 20	−25	97	1.93	1.07	4.0	4.2	99	0.49	-2.28	4.4	3.1
529	0 40	−25	99	1.50	-1.23	4.3	4.4	101	0.67	-2.28	3.6	3.1
530	1 00	−25	92	1.48	0.01	3.4	3.5	99	1.71	1.06	3.3	3.2
531	1 20	−25	88	1.33	-0.73	2.9	3.1	92	-0.83	0.04	3.2	2.5
558	10 20	−25	80	1.17	0.52	3.8	3.4	82	-0.32	-2.28	3.3	3.5
567	13 20	−25	71	—	—	4.0	4.9	79	1.28	-4.52	3.2	3.2
598	23 40	−25	77	-0.14	-0.20	4.1	4.1	80	-2.82	-0.87	3.8	3.6
702	10 20	−15	67	-1.48	-2.56	3.9	5.4	66	-2.05	-3.68	3.2	2.8
737	22 00	−15	72	0.34	-1.38	3.3	3.8	72	-0.23	0.46	3.0	3.6

– To derive the absolute proper motions, the mean weighted reflex proper motion of galaxies is subtracted from all proper motions. Finally, the absolute proper motions are aligned with the celestial coordinate system defined by the PPM Star Catalogue (Bastian et al. 1993) in its B1950 representation. (The final SPM Catalog will be on the Hipparcos system).
– The SPM proper motions for the Hipparcos stars are calculated as a weighted mean from all available absolute proper motions (from different exposures, grating-image orders and overlapping SPM fields when applicable). The weights are estimated from a scatter around the mean for each image system.

3.2. Hipparcos catalogue link stars

For the purpose of the Hipparcos proper-motion link about 4100 HIC stars have been measured in 63 SPM fields. The distribution of the Hipparcos stars is shown in Fig. 2 for both the SPM and NPM. The SPM fields can be recognized as the densely 'populated' areas. The SPM field centers are given in Table 2 along with the number of measured Hipparcos stars (N_H) on the blue and visual plate-pairs. Since many SPM fields have overlap with adjacent fields, a fairly large number of HIC stars have 2 to 4 independent determinations of absolute proper motion. The star was excluded from the solution if $|\Delta\mu_{H-SPM}| > 13$ mas yr^{-1} where 'H' denotes Hipparcos proper motions. As in the case of the NPM solution the Hipparcos proper motions were transformed to the B1950 equator.

The mean number of reference galaxies per field is 250 on blue plates (SPM_B) and 190 on visual plates (SPM_V) yielding a mean uncertainty in the correction to absolute proper motions of 1.0 mas yr^{-1} for each field. Since the Hipparcos stars are represented by several images per star (ten in the most favourable case) the proper motion accuracy in each color (blue or visual) can be as good as 2 to 3 mas yr^{-1}. The blue and visual plate-pairs are essentially independent which provides one means of error estimate. Double exposure and grating images supply another means of checking the proper-motion accuracy, as do the overlap regions of adjacent fields. The standard error σ of the link solution characterizes the external error of the SPM proper motions. Knowing the Hipparcos proper-motion accuracy in our sample (about 1.0 mas/yr in each component), the external accuracy of the SPM proper motions for bright stars is 3 to 4 mas yr^{-1}.

The SPM link solutions are given in Table 1. The mean-per-field spin post-fit residuals, $\langle\Delta\mu\rangle_{H-SPM}$, in both colors and coordinates along with standard errors, σ_α and σ_δ, of the $\langle\Delta\mu\rangle$ are listed in Table 2. If $|\langle\Delta\mu\rangle_{H-SPM}|$ exceeds ≈ 3.5 mas yr^{-1} that entry is omitted in Table 2 and not used in the link solution.

If the standard errors given in Table 2 were composed entirely of random measurement and modeling errors, the precision of each spin component with the given number of Hipparcos stars in hand could be in the range of 0.1 to 0.2 mas yr^{-1}. However, the spin solutions from Table 1 indicate somewhat larger scatter in the spin components when compared to this precision estimate and also show a noticeable offset in the ω_y component with respect to the adopted solution (Kovalevsky et al. 1997). In what follows, we attempt to give an interpretation of these effects.

The SPM reductions include two steps which may shift the absolute proper motions of an entire field. These are the correction for the magnitude equation and the zero-point correction to absolute proper motions. The latter is known to $\approx \pm 1$ mas yr^{-1}. This uncertainty acts in a systematic way as an offset akin to the modelling error in the plate solution. Hence, this offset will affect all proper motions in the field. This would argue that the fields should be weighted equally and not by the number of Hipparcos stars they contain. In practice, the number of Hipparcos stars, N_H, is nearly constant from field to field (Table 2) and thus the effect is minimal. To substantiate this assumption a solution was made using the average proper-motion differences $\langle\Delta\mu\rangle_{H-SPM}$ per field. Equal weights were assigned to all fields. The corresponding spin solutions are given in Table 3 where the content of the columns is the same as for Table 1 except for N_f which denotes the number of SPM fields used in the solution. A field was excluded from the solution if $|\langle\Delta\mu\rangle_{H-SPM}| > 3$ mas

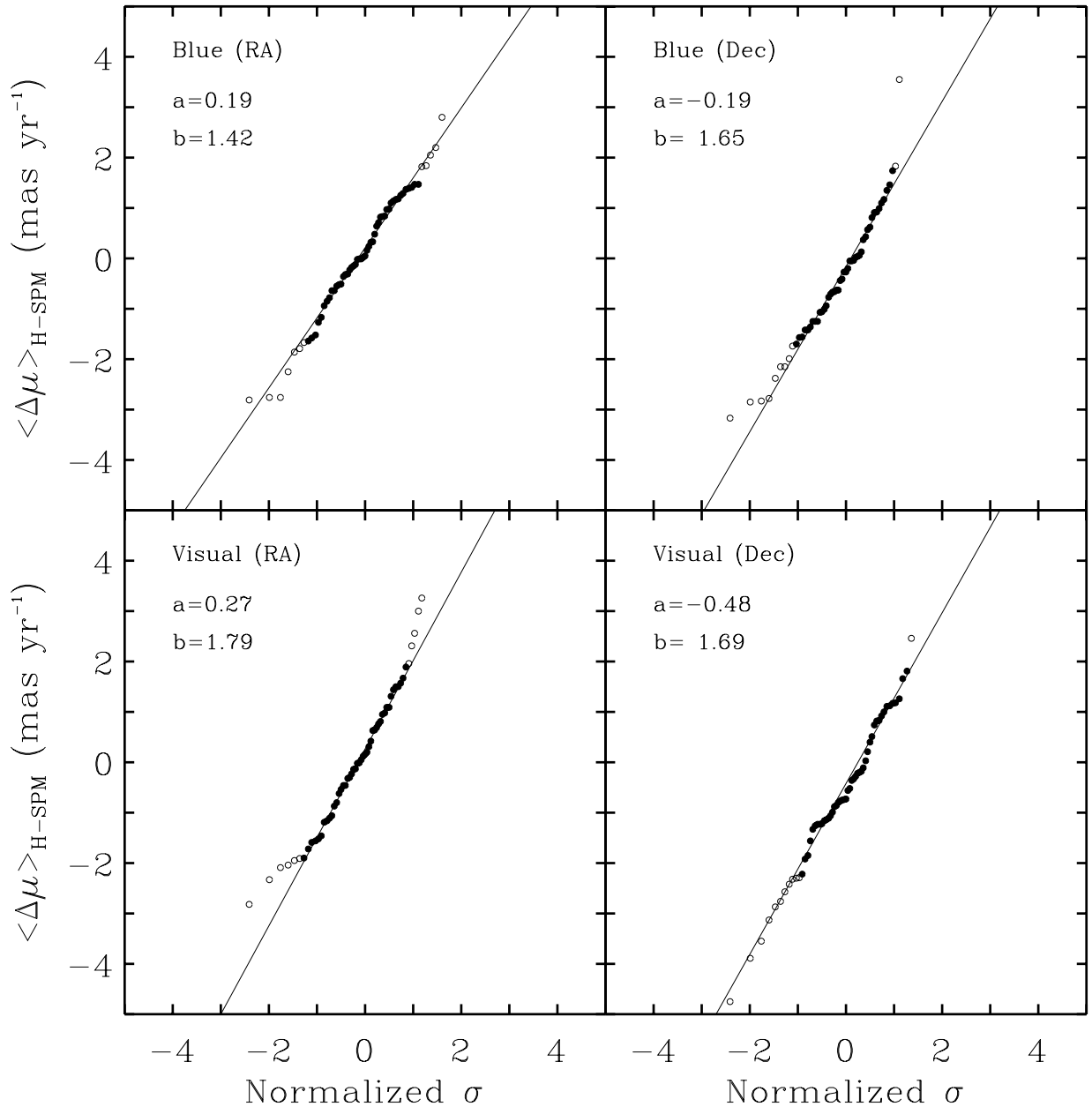

Fig. 3. Normalized probability plots of the post-fit Hipparcos *minus* mean-per-field SPM proper motions. The differences from blue plates are plotted in the upper two panels; the visual plates are shown in the lower panels. All four plots indicate a standard deviation of ∼1.6 mas yr^{-1}. Note an offset in the proper-motion differences for the visual plates most likely due to a residual magnitude equation. The fit of a straight line was calculated using the central 80% of the data which are denoted by bold dots. The intercept (a) and slope (b) of that line are indicated in the upper left corner of each panel.

yr^{-1}. As expected the spin-component values are close, albeit not identical to these from the solution with individual stars. The errors of the spin components have a three-fold increase over similar ones in Table 1. Actually, the formal error estimates in Table 3 are much closer to the adopted error values in the final synthesis (Kovalevsky et al. 1997). This is pointing to the field-to-field proper motion shifts for which it will be shown a major contributor is a residual magnitude equation.

We present the correlation matrix $C^{\rm S}$ for the right ascension solution from the blue SPM plates (fifth line in Table 1). It shows moderate correlations which are a result of the uneven distribution of the SPM fields. The order of the elements in matrix $C^{\rm S}$ follows the term sequence ω_x, ω_y and ω_z.

$$C^{\rm S} = \begin{pmatrix} 1.00 & -0.17 & -0.38 \\ & 1.00 & -0.16 \\ & & 1.00 \end{pmatrix} \quad (3)$$

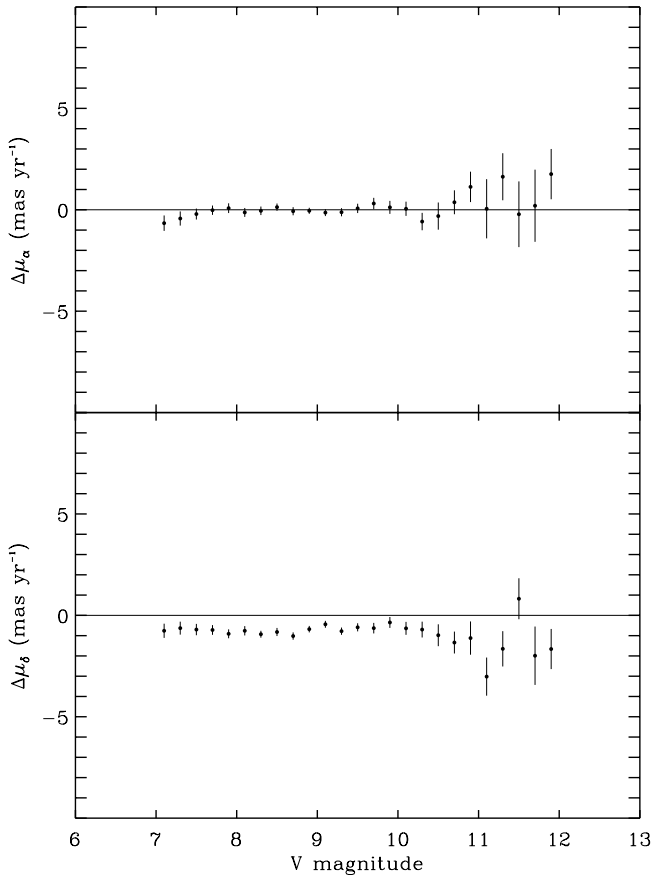

Fig. 4. Binned Hipparcos (H) *minus* SPM proper motions from visual plates as a function of V magnitude. Error bars represent error of the mean in each magnitude bin. The offset in $\Delta\mu_\delta$ plot probably is due to the magnitude equation.

3.3. Magnitude equation in SPM plates

The critical part of the reduction procedure (Sect. 3.1) is correcting for the magnitude equation. Initial comparisons between the H37C and SPM preliminary data showed that in some fields the magnitude equation can produce a spurious offset in proper motions reaching several mas yr^{-1}. The same pattern was observed in direct comparisons of the preliminary Hipparcos and SPM star positions (Platais et al. 1995). This clearly pointed to the presence of significant magnitude equation in the SPM coordinates and proper motions. In general, it is assumed that the correction for magnitude equation is a function of a star's magnitude and position on the plate. One expects the magnitude equation to gradually decrease towards the fainter magnitudes and vanish for images having instrumental magnitudes close to the plate limit.

The great advantage of the SPM plates over other similar survey-plates is the availability of grating images for stars at different apparent magnitudes. The key assumption is that the magnitude equation effects the central (zero order) and higher order grating images in the same fashion, i.e. from the grating-image positional differences it is possible to obtain absolute offsets in coordinates for all stars (Jefferys, 1962). These offsets are not necessarily the same in the long and short exposure images, hence, they require separate corrections.

Thus, the bulk of the magnitude equation in coordinates and proper motions can be removed using the grating-image offset modelling technique formulated by Jefferys (1962) and adapted to the SPM plates by Girard et al. (1998). The application of this technique to the SPM plates allowed us to lower the contribution of magnitude equation in proper motions to about a few tenths of mas yr^{-1}. Further improvements are hindered rather by nature since the number of stars at the bright end cannot be increased and the magnitude equation may have a complicated pattern too difficult to model adequately. For the faint stars the magnitude equation cannot be established very well either due to the considerable scatter in the grating-image differences. In addition, the magnitude equation in the SPM plates is stronger and more complex in declination (Platais et al. 1995, Girard et al. 1998). Such a disparity in the magnitude equation appearance suggests that a spin solution using the proper-motion differences in right ascension could be less prone to the magnitude-effect related systematics.

Table 3. Residual spin components from the mean-per-field SPM-data solution

Data	$\Delta\mu$	$\omega_x \pm \epsilon_x$	$\omega_y \pm \epsilon_y$	$\omega_z \pm \epsilon_z$	N_f	σ
SPM_B	$\mu_\alpha \cos\delta$	+0.19±0.37	+0.72±0.58	–0.03±0.22	60	1.3
SPM_V	$\mu_\alpha \cos\delta$	+0.34 0.43	+0.85 0.70	–0.20 0.27	58	1.5
SPM_B	μ_δ	-0.03 0.46	+0.61 0.21	—	56	1.4
SPM_V	μ_δ	+0.27 0.50	+0.73 0.25	—	60	1.6
SPM_B^a	$\mu_\alpha \cos\delta$	+0.11 0.33	+0.47 0.51	–0.12 0.20	60	1.1
SPM_V^a	$\mu_\alpha \cos\delta$	+0.20 0.36	+0.24 0.58	–0.02 0.22	58	1.2
SPM_B^a	μ_δ	0.03 0.39	+0.33 0.17	—	56	1.2
SPM_V^a	μ_δ	+0.20 0.44	+0.59 0.22	—	60	1.4

[a] Galaxy magnitudes modified & magnitude equation re-calibrated

3.4. Verification of post-fit residuals

There are several ways to test the Hipparcos-SPM spin post-fit residuals for the presence of systematic errors. Firstly, it is useful to check for normality of the distribution of the mean, field-to-field, residual differences. The so-called cumulative probability plots (cf. Lutz & Upgren 1980) of these residuals indicate a relative closeness to a normal distribution with standard deviation around 1.6 mas yr^{-1} (Fig. 3). There is, however, a significant offset in the visual-plate proper motions in declination ($\langle\Delta\mu_\delta\rangle$ = −0.5 mas yr^{-1}). Most likely this offset is caused by a residual magnitude equation.

The next test, the binned post-fit residual distribution as a function of magnitude (Fig. 4), shows no significant magnitude dependence. However, the whole set of residuals in declination is shifted by 0.7 mas yr^{-1} for visual plates and by 0.4 mas yr^{-1}

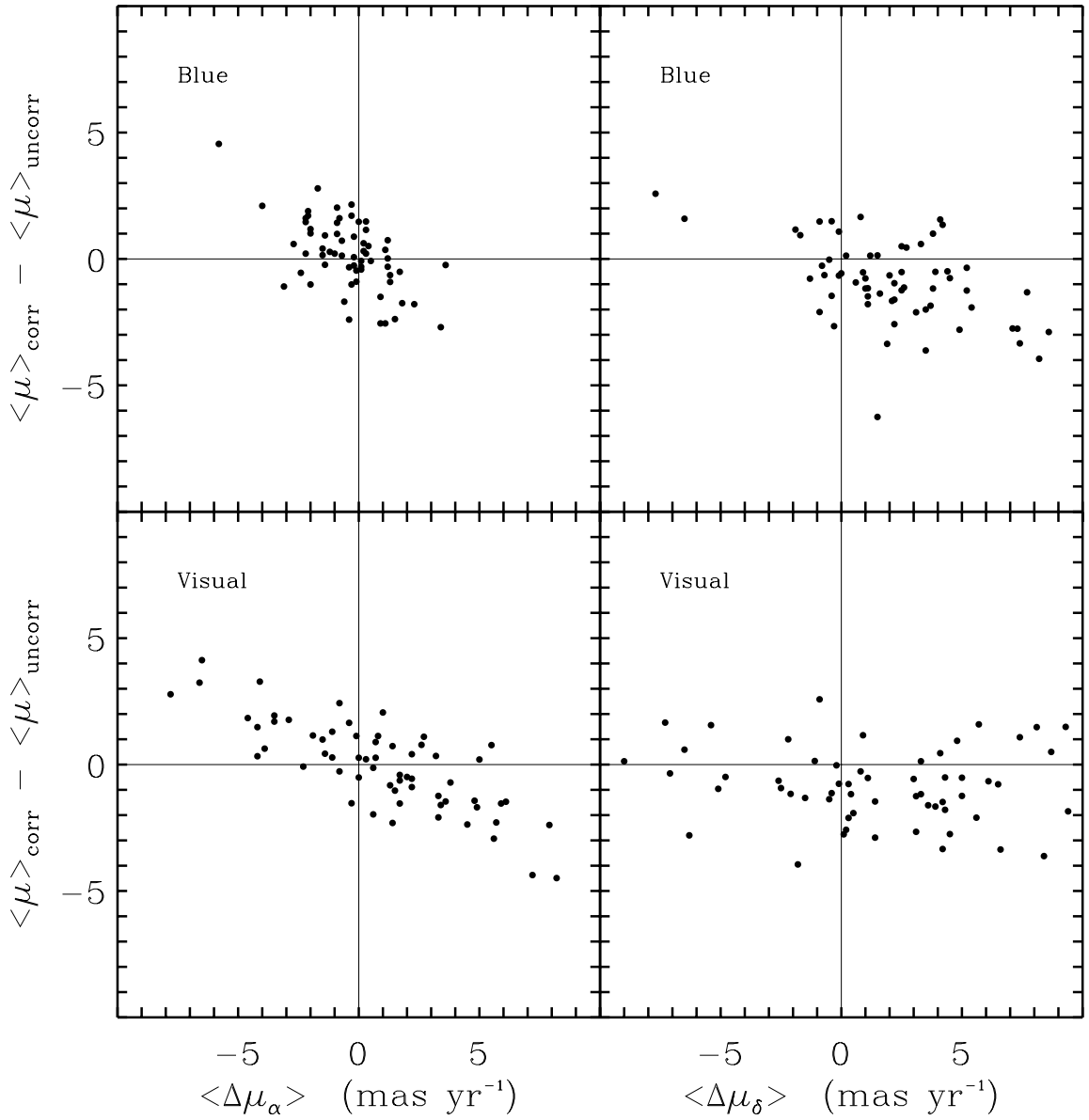

Fig. 5. Mean-per-field differences, Hipparcos (H) *minus* SPM proper motions, as a function of the amount of magnitude equation correction applied in the SPM reductions. The panel arrangement is similar to Fig. 3.

for blue plates, as already indicated by the probability plots (Fig. 3). A variety of plots showing residuals as a function of right ascension, declination, inner or outer part of the field and color did not produce any meaningful evidence for any other systematic errors.

It had been noticed earlier that the fields requiring a large magnitude-equation correction frequently produce rather large mean-per-field residuals. This effect is seen in Fig. 5 where we plot the mean magnitude-equation applied for each field as a function of Hipparcos *minus* corrected SPM proper motions for the blue and visual plates separately. Apparently, there is a non-negligible correlation between the corrections applied and $\langle\Delta\mu\rangle_{\rm H-SPM}$ differences. As reasoned by Girard et al. (1998) the amount of magnitude-equation correction is also similarly correlated with the zero-point corrections to absolute proper motion. The latter correlation strongly suggests that galaxies might have a magnitude equation different from that affecting the stellar images.

It is not possible, however, to calibrate the magnitude equation from galaxies alone, therefore, an empirical procedure was adopted (Girard et al. 1998) which changes the magnitudes of galaxies by a certain amount *before* applying the magnitude equation corrections. A minimization of trends in the differences in zero-point correction to absolute proper motions derived from blue- and visual-plate pairs suggests a correction to the galaxy magnitudes of $\Delta m_{\rm g} = -0.7$ mag. Although this adjustment of galaxy magnitudes is essentially empirical, there is a good reason to suspect that the magnitudes of galaxies are consistently

underestimated. It has been noticed (Platais et al. 1993) that the galaxy magnitudes are very sensitive to the centering algorithm used and may differ by up to several (!) magnitudes for the very bright ones. Our scale of galaxy magnitudes is close to the COSMOS/UKST Object Catalog (Yentis et al. 1992) which yields much fainter magnitudes with respect to the Guide Star Catalog galaxy magnitudes. Since the modified galaxy magnitudes are narrowing this gap, they possibly can be considered as more reliable.

The modified spin solutions using a re-calibrated magnitude equation as explained above are given in Table 3. The solutions were obtained using the mean-per-field 'H − SPM' differences. One can readily notice an improvement in the link solution: all errors are smaller and, most important, the mean value of ω_y has dropped almost two times with respect to all previous rather peculiar ω_y values (see also Platais et al. 1997). Apparently, our diagnosis for the spin component offsets, i.e. the residual magnitude equation effect, is correct. However, even after the re-calibration of galaxy magnitudes some small and variable field-to-field residual magnitude equation still persists in the SPM data (Girard et al. 1998). Hopefully, with the accumulation of a much larger sample of SPM fields it will be possible to considerably reduce the influence of this residual magnitude equation on the link solution.

4. Conclusions

In total the NPM and SPM programs furnished ∼13,000 stars for the Hipparcos proper-motion link to the extragalactic reference system. Both programs have demonstrated their ability to provide precise spin components if the magnitude equation, present in the NPM and SPM data, is accounted for. The SPM link solution alone (using the data as of February 1996) indicates that the Hipparcos proper-motion system is rotating no more than ∼0.2 mas yr^{-1}. It is expected that upon completion of the SPM program the link solution can be improved by a factor of five in accuracy.

It seems that the NPM proper motions of bright Hipparcos stars could be corrected for the magnitude equation *globally*, i.e., by applying one magnitude equation correction to all stars in the NPM1 Catalog. For this purpose we need some external and free of magnitude equation proper-motion catalogue. Currently no such catalogue, except the Hipparcos Catalogue itself, is available. The Lick astrometry group, however, intends to re-examine all brighter stars and the link problem shortly. Thus, the NPM solutions and approaches presented here have to be considered as exploratory and preliminary.

The SPM data indicate a different pattern of magnitude equation. There are no signs of a global magnitude equation (if an offset in μ_δ is neglected), however, individual fields may have significant residual magnitude equation. Since the SPM fields used in the link solution are not distributed evenly, such residual magnitude equation can easily create a spurious rotation effect. We believe that the peculiar ω_y value in the SPM solutions is due to a residual magnitude equation. Further investigation into the matter showed that possibly galaxies have been undercorrected for the magnitude equation. It was found that before the application of magnitude-equation correction the galaxy magnitudes should be brightened by 0.7 mag. The positive effect of this procedure is evident. The formal error estimates appear to be more realistic if the link solution is made by using mean-per-field differences $\langle\Delta\mu\rangle_{\mathrm{H-SPM}}$ and, thus, depends on the total number of fields rather than stars.

To the reader the present analysis of the magnitude equation may appear to be over-emphasized. In fact, the superb Hipparcos data have highlighted this problem in photographic astrometry with an unprecedented clarity, thus, forcing us to re-examine all large position and proper-motion surveys. We expect that our experience will alert others to check for possible magnitude equation in photographic surveys targeted towards galactic kinematic studies because even a small offset in the proper motions can seriously bias the results of Galaxy modeling, especially for the fainter, more distant stars which are not covered by the Hipparcos mission.

Acknowledgements. We thank W.-Z. Ma and T.-G. Yang for their help with measurements in the early stages of the SPM program. The SPM program is supported by grants from the U.S. National Science Foundation to Yale University and the Yale Southern Observatory, Inc. The Lick NPM program is also supported by grants from the U.S. National Science Foundation. This research has made use of the Simbad database operated at CDS, Strasbourg, France.

References

Bastian U., Röser S., Yagudin L.I., et al., 1993, PPM Star Catalogue, Vol. III-IV, Astronomisches Rechen-Institut, Heidelberg
Girard T.M., Platais I., Kozhurina-Platais V., van Altena W.F., López C.E., 1998, AJ (in press)
Jefferys W.H., 1962, AJ, 67, 532
Klemola A.R., Vasilevskis S., Shane C.D., Wirtanen C.A., 1971, Publ. Lick Obs., 22, Pt. II, 1
Klemola A.R., Jones B.F., Hanson R.B., 1987, AJ, 94, 501
Klemola A.R., Hanson R.B., Jones B.F., 1993, Lick Northern Proper Motion Program: NPM1 Catalog, Astronomical Data Center catalog No. A1199
Klemola A.R., Hanson R.B., Jones B.F., 1994, Galactic Astrometry: Observation & Application. In: Morrison L.V., Gilmore G.F. (eds.) Galactic and Solar System Optical Astrometry. Cambridge University Press, p. 20
Kovalevsky J., Lindegren L., Perryman M.A.C., et al., 1997, A&A, 323, 620
Lasker B.M., Sturch C.R., López C.E., et al., 1988, ApJS, 68, 1
Lindegren L., Kovalevsky J., 1995, A&A, 304, 189
Lutz T.E., Upgren A.R., 1980, AJ, 85, 1390
Platais I., Girard T.M., Méndez R.A., et al., 1992, Contributed Papers. In: Heck A., Murtagh F. (eds.) ESO Conference & Workshop Proc. No. 43, Astronomy from Large Databases II, p. 455
Platais I., Girard T.M., van Altena W.F., López C.E., 1993. In: Davis Philip A.G., Hauck B., Upgren A.R. (eds.) Workshop on Databases for Galactic Structure. L. Davis Press, Schenectady NY, p. 153
Platais I., Girard T.M., van Altena W.F., et al., 1995, A&A, 304, 141
Platais I., Kozhurina-Platais V., Girard T.M., et al., 1997. In: Hipparcos Venice '97, ESA SP-402. ESTEC, Noordwijk, p. 153
Turon C., Crézé M., Egret D., et al., 1992, The Hipparcos Input Catalogue, ESA SP-1136. ESTEC, Noordwijk

van Altena W.F., Girard T., López C.E., López J.A., Molina E., 1990, Realization and Comparison of Reference Frames. In: Lieske, J.H., Abalakin V.K. (eds.) Proc. IAU Symp. 141, Inertial coordinate system on the sky. Kluwer Acad. Publ., Dordrecht, p. 419

Yentis D.J., Cruddace R.G, Gursky H., et al., 1992, Digitisation Programmes – Current and Planned. In: MacGillivray H.T., Thomson E.B. (eds.) Digitised Optical Sky Surveys. Kluwer Acad. Publ., Dordrecht, p. 67

This article was processed by the author using Springer-Verlag LaTeX A&A style file *L-AA* version 3.